

## Original Article

# FTIR Spectroscopic Comparison of Fish Scale Collagen and Acemannan-Modified Porcine Collagen for Oral Mucosal Scaffolds

Orakarn Kanwiwatthanakun<sup>1</sup>, Utaisar Chunmanus<sup>2</sup>, Ratsa Sripirom<sup>3</sup>, Pasutha Thunyakitoisal<sup>3</sup>

<sup>1</sup>Children's Oral Health Department, Institute of Dentistry, Suranaree University of Technology, Nakhonratchasima, Thailand

<sup>2</sup>Laboratory Scientist 2, Food and Agriculture Research Section (FRS), Synchrotron Research and Applications Division (SRD), Synchrotron Light Research Institute (Public Organization), Thailand

<sup>3</sup>Institute of Dentistry, Suranaree University of Technology, Nakhonratchasima, Thailand

## Abstract

Oral mucosal defects, especially in elderly patients with cancer, trauma, or post-surgical resections, require biomaterials that are biocompatible, promote tissue regeneration, and restore function. Collagen-based scaffolds are extensively researched due to their biocompatibility and structural similarities to natural tissue. However, characterizing the molecular integrity of these scaffolds is essential for ensuring their efficacy. This pilot study employed Fourier transform infrared spectroscopy (FTIR) as a fundamental analytical tool to investigate and compare two collagen-based scaffolds system as two distinct modification strategies: (1) fish scale-derived collagen crosslinked with 1-ethyl-3-(3-dimethylaminopropyl) carbodiimide (EDC) and (2) porcine skin-derived collagen coated with acemannan (AceCol). FTIR was used to investigate structural features, specifically the maintenance of collagen's triple-helix structure (Amide I-III bands) and the integration of bioactive polysaccharide groups. The spectra was analyzed for key vibrational peaks, such as hydroxyl (O-H), amide, and polysaccharide-specific regions. The results indicate that the EDC-crosslinked fish scale collagen scaffold exhibited intact Amide I-III bands, confirming the stability of the triple-helix structure. The acemannan-coated scaffold displayed additional peaks in the range of 1000–1100 cm<sup>-1</sup> and enhanced hydroxyl band intensity (3300–3400 cm<sup>-1</sup>), which indicates successful polysaccharide integration. In conclusion, this pilot study demonstrated that FTIR spectroscopy can differentiate structural signatures between two scaffold modification strategies. EDC crosslinking retained the triple-helix stability of fish scale-derived collagen, while acemannan coating introduced polysaccharide-related features in porcine collagen. These findings provide preliminary evidence supporting the complementary roles of crosslinking for stability and coating for bioactivity, warranting further validation for future applications in oral mucosal regeneration.

**Keywords:** Acemannan, Fish-scale collagen, FTIR, Oral tissue engineering

**Received date:** Jul7, 2025

**Revised date:** Sep 3, 2025

**Accepted date:** Sep 9, 2025

**Doi:** 10.14456/jdat.2025.24

**Correspondence to:**

Orakarn Kanwiwatthanakun, Children's Oral Health Department, Institute of Dentistry, Suranaree University of Technology, Nakhonratchasima, Thailand. Tel 0-4422-3592 Email: s\_orakarn@sut.ac.th

## Introduction

Elderly patients, particularly those suffering from cancer, trauma, or following surgical resection, frequently

have oral mucosal defects.<sup>1</sup> These defects can significantly affect many functions, such as speech, mastication, aesthetics,

and overall quality of life.<sup>2</sup> Therefore, the development of effective and biocompatible scaffolds is essential to support tissue regeneration and restore oral function.<sup>3</sup> Current treatments, like autologous grafts, have limitations due to donor site morbidity, low tissue availability, and unpredictable healing outcomes.<sup>4</sup> This situation has driven the development of tissue-engineered biomaterials that can mimic the structural and biological properties of native oral mucosa.<sup>5</sup> Among the various candidates, collagen-based scaffolds have gained considerable attention due to their favorable properties for soft tissue regeneration.<sup>6</sup> These properties include biocompatibility, biodegradability, low immunogenicity, and structural similarity to the native extracellular matrix.<sup>7</sup>

Comprising about thirty percent of all the proteins in the body, collagen is the main structural protein found in mammals, which is an essential component that provides mechanical strength to connective tissue, including skin, bone, and cartilage.<sup>8</sup> The fundamental structural unit of collagen consists of three polypeptide chains: two identical  $\alpha 1$  chains and one slightly variant  $\alpha 2$  chain, which are intertwined in a unique triple-helical shape. This structure consists of a repeating sequence of amino acids called glycine-X-Y (Gly-X-Y), with X and Y often being proline and hydroxyproline. The stability of the triple helix is mostly maintained by hydrogen bonding between adjacent carbonyl (CO) and amine (NH) groups.<sup>9</sup> Additionally, the unique physical properties of collagen, including high water absorption, gel-forming ability, and surface activity at lipid-free interfaces, make it a versatile material for biomedical applications such as scaffolds, wound-healing material devices, and drug delivery systems.<sup>7-8</sup>

Traditionally, mammalian by-products, such as bovine and porcine tissues, have been the primary source of collagen for medical and industrial applications. However, increasing concerns about zoonotic infectious disease transmission, allergenicity, ethical considerations, and religious restrictions have inspired much research into safer and more sustainable alternative sources.<sup>10</sup> Recently, researchers have focused on thousands of tons of by-products, including fish bones, skin, and scales, which are typically food waste from human consumption, as alternative

sources of collagen.<sup>11</sup> Among these, fish scales are gaining more interest due to their natural qualities that resemble type I collagen, which is composed of two  $\alpha 1$  chains and one  $\alpha 2$  chain<sup>12</sup> and is found in over 90% of the human body<sup>13</sup> within nearly all extracellular matrix and connective tissues.<sup>8</sup> In addition, collagen from fish scales demonstrates proper water absorption and retention properties, which makes it appropriate for the creation of biomedical scaffolds.<sup>14</sup> However, compared to mammalian collagen (39–40°C), collagen derived from fish scales typically has a lower denaturation temperature (Td), around 35–36°C, which limits its use in biomedical applications.<sup>13,15</sup> The lower levels of proline and hydroxyproline in marine collagen, which are essential for hydrogen bonding to stabilize the triple-helix structure, are the main cause of this decreased thermal stability.<sup>7,16</sup> Consequently, collagen derived from fish denatures at temperatures close to physiological values, which presents a major challenge for *in vivo* applications.<sup>12</sup> To overcome this limitation, researchers have employed several physical and chemical crosslinking methods to enhance the structural integrity of fish collagen.<sup>17</sup> Among different crosslinking methods, chemical crosslinking is considered the most suitable for type I collagen-based scaffolds, as it enhances scaffold stability without causing structural changes. Notably, 1-ethyl-3-(3-dimethylaminopropyl) carbodiimide (EDC) stands out as a zero-length crosslinker that enhances mechanical strength and thermal stability without leaving toxic residues or significantly altering the native structure.<sup>18</sup>

Recent studies have also explored the functionalization of collagen scaffolds with bioactive molecules.<sup>19</sup> Acemannan is a significant natural polysaccharide derived from the inner gel of *Aloe vera*. It is a highly acetylated polysaccharide consisting of  $\beta$ -(1,4)-linked mannose units.<sup>20</sup> In previous studies, acemannan demonstrates excellent biocompatibility and biodegradability, along with immunomodulatory, antiviral, antitumor, and antioxidant properties, making it highly suitable for biomedical applications.<sup>21-23</sup> Additionally, it stimulates wound healing, matrix formation, and cell proliferation.<sup>24</sup> Spectroscopic techniques can investigate interactions between its acetylated polysaccharide structure

and the polypeptide chains of collagen.<sup>24</sup> However, to the best of our knowledge, no study has directly compared fish scale-derived collagen crosslinked with EDC and porcine skin-derived collagen functionalized with acemannan using the same analytical framework. This lack of comparative evidence represents a critical knowledge gap, particularly in understanding how scaffold origin (marine vs. mammalian) and modification (crosslinking vs. coating) affect their structural and functional characteristics.

Fourier transform infrared (FTIR) spectroscopy is a vibrational spectroscopic technique employed to investigate molecular-level alterations and identify chemical functional groups, types of chemical bonds, and molecular configurations.<sup>25</sup> Researchers have extensively utilized the FTIR spectroscopy to analyze protein structures and molecular interactions.<sup>26</sup> In the context of collagen, the Amide I band (1600–1700  $\text{cm}^{-1}$ ) primarily results from the stretching vibrations of C=O bonds in the peptide backbone. This band is recognized as a fundamental indicator of the triple-helical conformation and secondary structure of collagen (protein secondary structure elucidation using the FTIR spectroscopy). Additionally, the Amide II band (1470–1570  $\text{cm}^{-1}$ ), which encompasses N–H bending and C–N stretching vibrations, as well as the Amide III band (1250–1350  $\text{cm}^{-1}$ ), which includes C–N stretching and N–H deformation, provides critical information regarding the presence of proteins and polypeptides, along with the stability of the triple-helix structure.<sup>27</sup> Recent technological developments have permitted FTIR data to be acquired with a spatial resolution of approximately 10 microns from small tissue sections, enabling precise structural characterization at the microscale, which is useful in tissue engineering and scaffold evaluation.<sup>28</sup> The FTIR spectroscopy will serve as an essential analytical tool for comparing the chemical structures and molecular arrangements of collagen-based scaffolds derived from different sources, including pure fish scale-derived collagen and porcine skin-derived collagen coated with acemannan.

Accordingly, this work was conducted as a pilot study to assess the feasibility of FTIR spectroscopy in characterizing and distinguishing two scaffold systems as two distinct modification strategies: (1) fish scale-derived

collagen crosslinked with EDC and (2) porcine skin-derived collagen coated with acemannan. The central research question was whether FTIR could reliably differentiate the molecular and structural features arising from crosslinking and bioactive coating. It was hypothesized that the scaffolds would exhibit distinct molecular and structural signatures detectable by FTIR, reflecting differences in crosslinking and bioactive functionalization. The findings are intended to provide preliminary evidence and foundational knowledge that will guide the future optimization of tissue-engineered oral mucosa scaffolds for the treatment and restoration of oral mucosal integrity in elderly patients.

## Materials and Methods

### *Preparation of fish scale-derived collagen scaffold crosslinked with EDC*

Circular collagen scaffolds (16 mm in diameter and 1 mm in thickness) were fabricated using 1.1% (w/v) type I atelocollagen extracted from tilapia fish scales (Collawind Co., Ltd., Niigata, Japan) crosslinked with 1.0% (w/v) 1-ethyl-3-(3-dimethylaminopropyl) carbodiimide hydrochloride (EDC) (Tokyo Chemical Industry, Tokyo, Japan) for structural stabilization following a previously published protocol with minor modifications.<sup>5</sup>

Briefly, freeze-dried collagen (Cell Campus FD-08G, Taki Chemical Co., Ltd., Hyogo, Japan) was dissolved in hydrochloric acid (pH 3.0) and mixed with Dulbecco's phosphate-buffered saline (D-PBS; KAC Co., Ltd., Kyoto, Japan) at 4 °C. The resulting solution was poured into silicone rubber molds (1.0 mm thickness; Azone Corporation, Osaka, Japan) with circular holes (16 mm diameter) and incubated at 25°C to induce fibrillogenesis.

After gelation, the scaffolds were chemically crosslinked by using 1.0% (w/v) EDC dissolved in 99.5% ethanol (Kishida Chemical). Crosslinking was performed by immersing the collagen gel in the EDC solution at a ratio of 100 mg EDC per 7.8 mg of collagen and incubated for 24 hours at room temperature.

After crosslinking, scaffolds were carefully removed from the molds and washed sequentially in 50% ethanol and D-PBS, each for 24 hours under gentle rotational stirring at room temperature. The scaffolds were

then sterilized using  $\gamma$ -irradiation and stored in D-PBS at 4°C until further use.

#### ***Preparation of Porcine Skin-Derived Collagen Scaffold Coated with Acemannan (AceCol Scaffold)***

Fresh porcine skin was obtained from a certified local supplier and processed within 24 hours. After hair removal, the skin was soaked in 70% ethanol for surface sterilization and thoroughly rinsed with normal saline. Collagen was extracted following a previous study.<sup>27</sup> Briefly, the skin was treated with 0.1 M NaOH at a 1:10 (w/v) ratio for 24 hours to remove non-collagenous proteins and lipids. The tissue was washed with ice-cold deionized water until reaching neutral pH, followed by incubation in 0.3 M acetic acid at a 1:15 (w/v) ratio with porcine pepsin (20,000 units/g of skin; Sigma-Aldrich, USA) for 24 hours at 4°C. After centrifugation at 5000 rpm for 20 minutes, the supernatant was collected and precipitated with ice-cold 3 M NaCl at 4°C overnight. The resulting precipitate was centrifuged at 5000 rpm for 30 minutes, dialyzed with deionized water (10x volume), freeze-dried, and stored in a desiccator.

Acemannan was extracted from Aloe vera (*Aloe barbadensis* Miller) leaves as previously described.<sup>22</sup> The outer skin of the leaves was removed, and the inner pulp was washed, homogenized, and centrifuged. The supernatant was precipitated with 100% ethanol at 4°C overnight, followed by collection and lyophilization for use. To fabricate the acemannan–collagen (AceCol) scaffold, freeze-dried porcine collagen was dissolved in 0.1 M acetic acid, while acemannan was dissolved in warm deionized water. The two solutions were mixed at a 1:0.4 (w/w) ratio and homogenized thoroughly.<sup>24</sup> The mixture was then lyophilized to form a scaffold structure. Finally, the scaffold was sterilized using  $\gamma$ -irradiation (Thailand Institute of Nuclear Technology, Nakhon Nayok, Thailand) and stored in a desiccator until further use.

#### ***Characterization Using the Fourier Transform Infrared (FTIR) Spectroscopy***

The FTIR microspectroscopy was employed to investigate the structural characteristics of the collagen-based scaffolds. Samples were embedded in an optimal cutting temperature (OCT) compound using aluminum foil

molds. The compound was allowed to partially solidify until it became opaque and was subsequently positioned horizontally and fully covered with additional OCT. The embedded specimens were rapidly frozen in liquid nitrogen, cryosectioned at –20°C to a thickness of 20  $\mu$ m, and prepared for spectral analysis.

Infrared spectra were acquired using a Bruker Tensor 27 FTIR spectrometer coupled with a Bruker Hyperion 3000 infrared microscope. Measurements were conducted in attenuated total reflectance (ATR) mode using a 15x objective and a 20x ATR lens, along with a high-sensitivity mercury cadmium telluride (MCT) detector. Spectra were recorded over the range of 3400–650  $\text{cm}^{-1}$ , which includes key functional groups such as Amide I, II, and III characteristic of collagen, at a spectral resolution of 4  $\text{cm}^{-1}$  with 64 scans per point. For each scaffold type, samples were prepared from three independent batches. From each batch, three specimens were analyzed, and spectra were collected from three randomly selected areas per specimen. This approach ensured that the spectral data captured both intra-sample and inter-batch variability, thereby enhancing the repeatability and validity of the investigation. The collected data were subsequently analyzed as described in the following section.

#### ***Data Analysis***

OPUS 7.5 software (Bruker Optics Ltd., Ettlingen, Germany) was used for analysis of all obtained spectra. The spectra underwent baseline correction, normalization, and subsequent processing by second derivative transformation to improve the resolution of overlapping peaks, particularly in the Amide I region (1600–1700  $\text{cm}^{-1}$ ), which is sensitive to the triple-helix structure of collagen. Characteristic absorption bands associated with Amide I (C=O stretching), Amide II (N–H bending and C–N stretching), and Amide III (C–N stretching and N–H deformation) were identified and compared between the scaffold groups. Additionally, characteristic peaks in the 1000–1100  $\text{cm}^{-1}$  region were monitored to identify the presence of polysaccharide-specific vibrations (e.g., C–O–C) indicative of acemannan incorporation. Spectra from multiple randomly selected regions of each scaffold sample ( $n = 3$  per group) were averaged to ensure reproducibility and representative

analysis. Comparative assessments between scaffold types focused on shifts in peak positions and changes in relative intensity to evaluate structural differences. Chemical identification and verification of functional groups were performed by comparing the processed spectra against reference data in the OPUS spectral library using the Library Search function.

## Results

### FTIR Spectral Analysis of Fish Scale-derived Collagen Scaffold Crosslinked with EDC

The FTIR spectroscopy is employed to identify functional groups and molecular structures of organic compounds, with each peak corresponding to the vibrational modes of specific chemical bonds. The Fourier Transform Infrared (FTIR) spectrum of collagen derived from fish scales and crosslinked with EDC (n=3 independent samples) revealed specific absorption peaks characteristic of Type I collagen, as illustrated in Figure 1: A notable peak was observed in the range of 3300–3400  $\text{cm}^{-1}$ , corresponding

to the stretching vibrations of O–H and N–H bonds. These absorption peaks are associated with bound water molecules that contain hydroxyl and amino groups within the collagen structure. A prominent peak of Amide I was identified in the range of 1650–1660  $\text{cm}^{-1}$ , representing the C=O stretching vibration of peptide bonds. This peak is a primary indicator of the secondary structure of collagen, particularly its triple-helix configuration. A clear Amide II peak was detected at 1550–1560  $\text{cm}^{-1}$ , associated with N–H bending and C–N stretching, which provides additional structural information about the protein. Amide III was identified by a peak in the range of 1230–1240  $\text{cm}^{-1}$ , which arises from C–N and N–H vibrations. This region is unique for the stability and integrity of the triple-helical structure of collagen. Furthermore, the retention of distinct Amide I, II, and III bands indicates that the EDC crosslinking process did not notably disrupt the native triple-helical structure of collagen. Figure 1 thus serves as the baseline spectrum of the EDC-crosslinked fish collagen scaffold, providing a detailed reference for its molecular integrity.

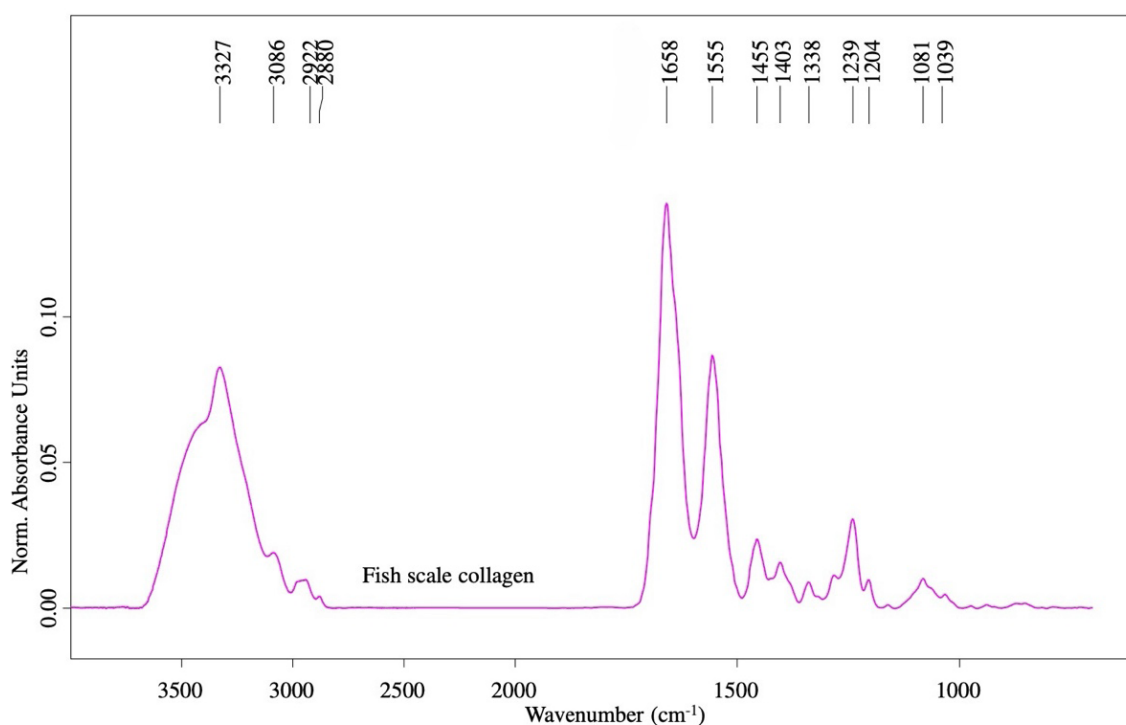


**Figure 1** FTIR spectrum of fish scale-derived collagen scaffold crosslinked with EDC. The spectrum shows the characteristic Amide I (~1650–1660  $\text{cm}^{-1}$ ), Amide II (~1500–1560  $\text{cm}^{-1}$ ), and Amide III (~1230–1240  $\text{cm}^{-1}$ ) bands, confirming the preservation of the triple-helix structure. A broad absorption band at 3300–3400  $\text{cm}^{-1}$  indicates O–H and N–H stretching vibrations associated with hydration and structural stability. This figure serves as the baseline spectral profile of the EDC-crosslinked fish collagen scaffold



### FTIR Spectral Analysis of Porcine Skin-Derived Collagen Scaffold Coated with Acemannan (AceCol Scaffold)

The spectrum of acemannan-coated collagen scaffold (AceCol) (Figure 2,  $n=3$  independent samples) demonstrated several distinct spectral modifications, indicating the integration of polysaccharide-based functional groups into the collagen matrix, compared to the FTIR spectrum of fish scale-derived collagen. The AceCol scaffold exhibited a wider and more distinct absorption peak in the range of  $3300\text{--}3400\text{ cm}^{-1}$ , associated with O–H and N–H stretching vibrations. The increased intensity in this region suggests a higher hydroxyl group content, likely attributable to the polysaccharide structure derived from Aloe vera, which is rich in hydroxyl functionalities. Importantly, a new absorption peak appeared at  $1737\text{ cm}^{-1}$ , corresponding to the C=O stretching vibration of acetyl ester groups. This peak serves as a molecular signature of acemannan, confirming the existence of acetyl substitutions in its polysaccharide backbone. The

presence of acemannan in the AceCol spectrum strongly supports its effective deposition onto the collagen surface, as uncoated collagen scaffolds typically lack absorption in this region. Notably, the Amide I ( $1642\text{ cm}^{-1}$ ), Amide II ( $1555\text{ cm}^{-1}$ ), and Amide III ( $1239\text{ cm}^{-1}$ ) bands remained present, suggesting that the acemannan coating did not interfere with the triple-helical structure of the collagen backbone. Additionally, notable spectral changes were observed in the range of  $1200\text{--}1000\text{ cm}^{-1}$ , corresponding to C–O and C–O–C stretching vibrations characteristic of sugar ring structures in polysaccharides. These signals were absent in the fish scale-derived collagen, supporting the successful surface modification of acemannan onto the collagen matrix and supporting the hypothesis that the coating process did not disrupt the original collagen framework but instead introduced additional functional groups. Figure 2 therefore provides the baseline spectrum of the acemannan-coated scaffold highlighting unique acemannan-associated features in addition to collagen bands.

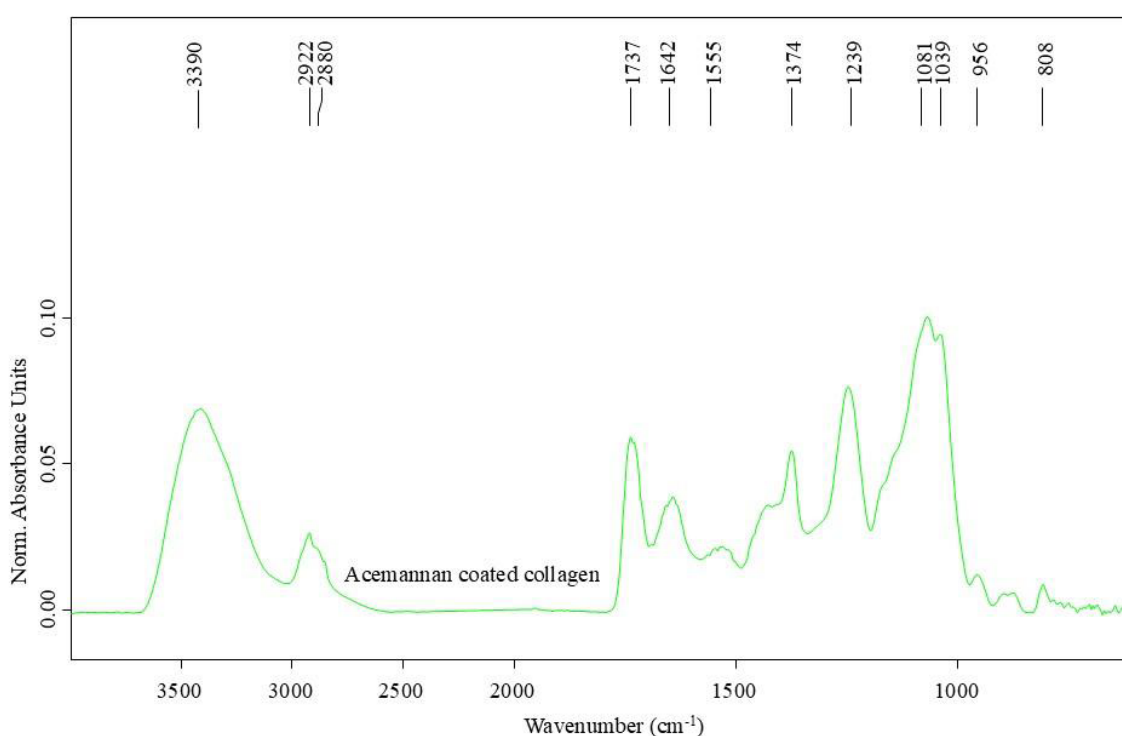


**Figure 2** FTIR spectrum of porcine skin-derived collagen scaffold coated with acemannan (AceCol). In addition to collagen-related amide bands, distinct peaks are observed at  $1737\text{ cm}^{-1}$  (C=O stretching of acetyl ester groups) and  $1000\text{--}1100\text{ cm}^{-1}$  (C–O and C–O–C stretching vibrations), representing molecular signatures of acemannan. The intensified absorption at  $3300\text{--}3400\text{ cm}^{-1}$  further reflects the hydroxyl-rich polysaccharide structure. This figure provides the baseline spectral profile of the acemannan-coated collagen scaffold, highlighting unique acemannan-associated features

### Comparison of FTIR Spectra for Two Types of Collagen Scaffolds

While Figures 1 and 2 present the baseline spectra of the individual scaffolds, Figure 3 overlays the two spectra to allow direct comparison between the modification strategies. Compared to fish scale collagen (purple line), the acemannan-coated scaffold (green line) exhibited stronger and more complex signals in the hydroxyl (3300–3400  $\text{cm}^{-1}$ ) and polysaccharide fingerprint (1200–1000  $\text{cm}^{-1}$ ) regions, as shown in Figure 3. Both samples

( $n=3$  independent spectra each) retained the major Amide I, II, and III bands, confirming the structural integrity of collagen in both scaffolds. The spectral differences indicate the successful surface modification of collagen with acemannan without disruption of its native conformation. Figure 3 thus provides a comparative overlay that highlights the structural stability of the fish collagen scaffold following EDC crosslinking and the successful incorporation of polysaccharide functional groups in the acemannan-coated scaffold.

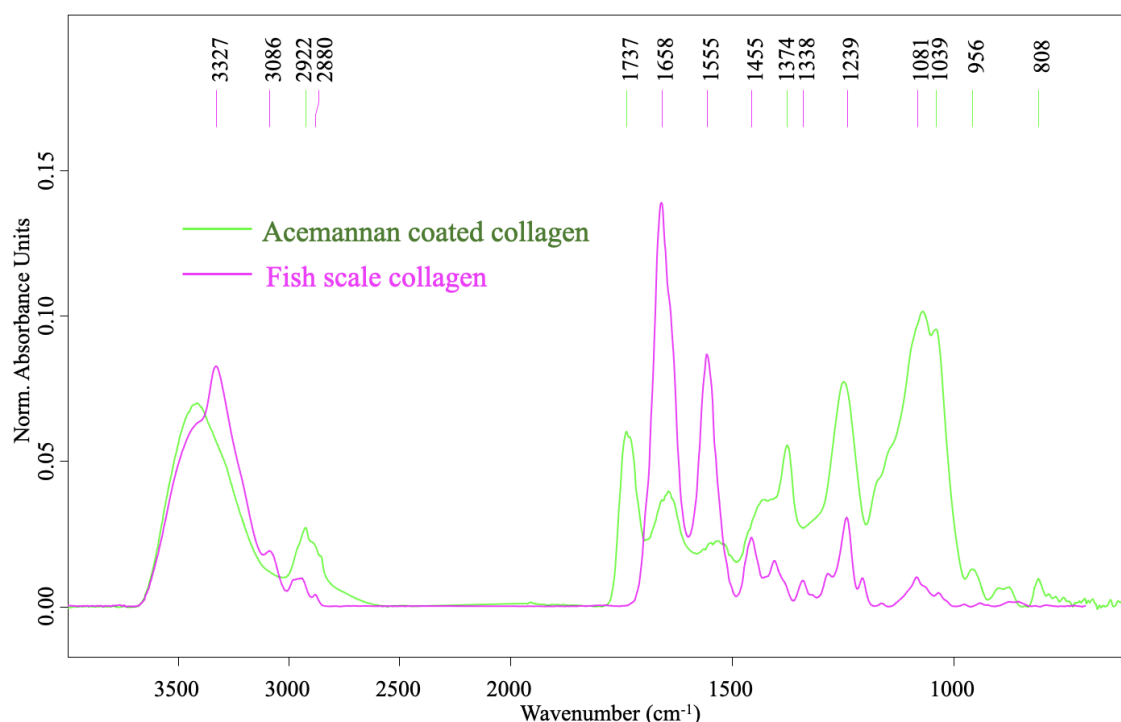


**Figure 3** Overlay of FTIR spectra of fish scale-derived collagen crosslinked with EDC (purple line) and acemannan-coated collagen (green line). The comparison highlights differences in the hydroxyl region (3300–3400  $\text{cm}^{-1}$ ) and polysaccharide fingerprint region (1200–1000  $\text{cm}^{-1}$ ), demonstrating the preservation of collagen's triple-helix structure alongside. The successful incorporation of acemannan functional groups. This figure provides direct comparative analysis of two scaffold modification strategies.

## Discussion

The Fourier Transform Infrared (FTIR) spectroscopy is a widely utilized technique for investigating the structural characteristics of biomaterials. Based on molecular vibrations, FTIR enables the identification of functional groups and secondary structures by detecting unique spectral fingerprints that reflect differences in atomic composition and molecular configuration.<sup>29</sup> This study aimed to characterize and compare the suitability of fish scale-derived collagen scaffolds crosslinked with EDC and porcine skin-derived collagen

scaffolds coated with acemannan for the development of oral mucosal tissue engineering using FTIR. The results validated the hypothesis that FTIR can detect distinct chemical and structural features in these scaffolds. The FTIR analysis of fish scale-derived collagen scaffolds revealed characteristic structural features corresponding to type I collagen, including well-defined peaks at Amide I (~1650–1660  $\text{cm}^{-1}$ ), Amide II (~1550–1560  $\text{cm}^{-1}$ ), and Amide III (~1230–1240  $\text{cm}^{-1}$ ), which are specific features of the triple-

helix structure typical of type I collagen. These peaks serve as key indicators of the secondary structure of protein.<sup>30</sup> In addition, a broad absorption band in the range of 3300–3400 cm<sup>-1</sup> was seen, corresponding to the vibrations of O–H and N–H bonds from hydroxyl and amino groups, as well as attached water molecules in the protein matrix.<sup>25</sup> This evidence suggests favorable water retention properties.<sup>8</sup> Previous studies have also reported that the surface hydrophilic groups, particularly O–H and N–H, can promote protein adsorption and integrin-mediated cell attachment, thereby contributing to enhanced cell adhesion.<sup>31</sup> However, FTIR alone cannot provide direct evidence of cellular responses, and future studies incorporating *in vitro* adhesion assays will be required to validate this interpretation. Moreover, these spectral findings align well with previous studies on marine-derived collagen, further supporting the reliability of FTIR in identifying triple-helix structures based on amide band signatures.<sup>32</sup> The retention of all three amide peaks (I, II, and III) after EDC crosslinking suggests that the triple-helix structure remained intact, which is a critical index for assessing the quality of scaffolds intended for oral mucosa tissue engineering.<sup>33</sup> These findings are consistent with several previous studies that recommend EDC as a suitable crosslinker for biomedical applications.<sup>34–37</sup>

In the acemannan-coated collagen scaffolds, increased absorption at 3300–3400 cm<sup>-1</sup> and new peaks at 1000–1100 cm<sup>-1</sup> indicated the presence of hydroxyl and polysaccharide functional groups. These findings confirm the successful incorporation of acemannan, which likely interacts with collagen through hydrogen bonding and electrostatic interactions. Importantly, the secondary structure of collagen remained unaffected, and all amide peaks were preserved (n=3 independent spectra).

While the principal Amide I, II, and III bands were preserved in both scaffolds, variations in their relative intensities were noted. In the acemannan-coated collagen scaffold, the Amide III band was more prominent relative to Amide I and II, while fish scale collagen exhibited a more balanced intensity pattern. This increased intensity of the Amide III signal, associated with C–N stretching and N–H bending, indicates preferred interactions between

acemannan and amino groups in collagen via hydrogen bonding and electrostatic interactions. These spectrum modifications indicate local environmental changes surrounding the collagen molecules without compromising the triple-helix structure, therefore supporting the notion that surface functionalization rather than backbone disruption occurred. In comparison to the collagen scaffold derived from porcine skin and coated with acemannan, an increase in absorption at 3300–3400 cm<sup>-1</sup> suggests the presence of abundant hydroxyl (–OH) groups in the acemannan structure.<sup>22</sup> Furthermore, notable changes were detected in the range of 1000–1100 cm<sup>-1</sup>, corresponding to the stretching vibrations of C–O and C–O–C bonds, which are characteristic of polysaccharides.<sup>25</sup> These changes indicate the presence of acemannan on the collagen surface. The detection of these polysaccharide-associated peaks provides qualitative evidence of successful acemannan coating; however, FTIR alone cannot be used to quantify the amount of coating, as peak intensity may vary with sample thickness, baseline correction, and local molecular environment. To determine coating levels more precisely, complementary methods such as thermogravimetric analysis (TGA), X-ray photoelectron spectroscopy (XPS), or biochemical assays would be required in future studies. This observation is consistent with other studies<sup>38–39</sup> that reported that acemannan interacts with biomaterials by hydrogen bonding and electrostatic interactions with amino groups in collagen. Importantly, the secondary structure of collagen remained unaffected, with all amide peaks preserved, therefore maintaining its triple-helix integrity, and making it appropriate for biomedical applications. This study also demonstrates that functionalization with acemannan introduces bioactive groups, such as hydroxyl and acetyl groups, which are known to support fibroblast proliferation and collagen production and promote wound healing.<sup>24,40</sup> This surface modification enhances bioactivity without compromising the native collagen structure, offering potential for biomedical applications, particularly for elderly patients with oral mucosal defects.

The FTIR analysis revealed the differences between fish scale-derived collagen and acemannan-coated collagen. The fish scale collagen retained its triple-helix integrity,



while the acemannan-coated collagen scaffold displayed additional functional groups specific to polysaccharides. These findings highlight a notable advantage of acemannan coating that could be applied in future applications for fish scale-derived collagen because, compared to collagen from mammalian sources, marine collagen provides advantages in terms of higher purity and greater ethical acceptability.<sup>12</sup> Coating fish collagen with acemannan may further improve its regenerative and anti-inflammatory properties and warrants further investigation. It should be emphasized that this work represents a pilot study, aiming to demonstrate the potential of FTIR as a primary tool for scaffold characterization. Another limitation of this study is the absence of reference scaffolds, such as uncrosslinked fish collagen or uncoated porcine collagen, which would have allowed more definitive comparisons. Including these controls in future work will help clarify whether the observed spectral features are specifically attributable to EDC crosslinking or acemannan coating. In addition, this study did not include quantitative spectral analysis (e.g., relative peak intensities or band area ratios), which would provide stronger comparative evidence. Future investigations will therefore incorporate such quantitative approaches to complement the present qualitative findings. While the findings indicate the potential of FTIR to distinguish between crosslinked fish collagen and acemannan-coated porcine collagen, relying solely on this single technique imposes limitations, as it cannot fully determine coating quantity, mechanical strength, or in vivo stability. The absence of complementary analyses also restricts the depth of interpretation. Therefore, future studies incorporating reference controls and additional techniques such as scanning electron microscopy (SEM), differential scanning calorimetry (DSC), thermogravimetric analysis (TGA), and mechanical testing are required to validate and expand upon these preliminary observations.

## Conclusion

In conclusion, this pilot study demonstrated that FTIR spectroscopy can effectively distinguish the molecular and structural features arising from two scaffold modification strategies. Fish scale-derived collagen

crosslinked with EDC retained its triple helix structure, confirming structural stability, whereas porcine skin-derived collagen coated with acemannan exhibited polysaccharide-related peaks, reflecting enhanced bioactivity. These findings provide preliminary evidence for the feasibility of FTIR in scaffold characterization and highlight the complementary potential of crosslinking for stability and coating for bioactivity. Further *in vitro*, *in vivo*, and clinical investigations, are warranted to validate these observations and guide the development of optimized biomaterials for oral mucosal regeneration in elderly patients.

## Acknowledgement

The authors would like to express their sincere gratitude to Professor Kenji Izumi of the Department of Biomimetics, Niigata University, Japan, for generously supplying the fish scale-derived collagen samples used in this study. We extend our sincere appreciation to the Synchrotron Light Research Institute (SLRI) in Thailand for providing access to the FTIR instrumentation and technical support for spectroscopic analysis. This research was financially supported by the Suranaree University of Technology (SUT), Thailand Science Research and Innovation (TSRI), and the National Science, Research, and Innovation Fund (NSRF) Grant number NRIIS 195680. The authors further confirm that this study did not involve the use of live animals. Fish collagen was obtained from a commercial source, and porcine skin was collected as a food by-product from a local market; therefore, approval from an animal ethics committee was not required.

## References

1. Bozdemir E, Yilmaz HH, Orhan H. Oral mucosal lesions and risk factors in elderly dental patients. *J Dent Res Dent Clin Dent Prospects* 2019;13(1):24-30.
2. Villanueva-Vilchis MD, López-Ríos P, García IM, Gaitán-Cepeda LA. Impact of oral mucosa lesions on the quality of life related to oral health. An etiopathogenic study. *Med Oral Patol Oral Cir Bucal* 2016;21(2):e178-84.
3. Izumi K, Yortchan W, Aizawa Y, Kobayashi R, Hoshikawa E, Ling Y, *et al*. Recent trends and perspectives in reconstruction and regeneration of intra/extra-oral wounds using tissue-engineered oral mucosa equivalents. *Jpn Dent Sci Rev* 2023;59:365-74.
4. Dean J, Hoch C, Wollenberg B, Navidzadeh J, Maheta B, Mandava

- A, *et al.* Advancements in bioengineered and autologous skin grafting techniques for skin reconstruction: a comprehensive review. *Front Bioeng Biotechnol* 2024;12:1461328.
5. Suebsamarn O, Kamimura Y, Suzuki A, Kodama Y, Mizuno R, Osawa Y, *et al.* In-process monitoring of a tissue-engineered oral mucosa fabricated on a micropatterned collagen scaffold: use of optical coherence tomography for quality control. *Heliyon* 2022;8(11):e11468.
6. She J, Liu J, Mu Y, Lv S, Tong J, Liu L, *et al.* Recent advances in collagen-based hydrogels: Materials, preparation and applications. *React Funct Polym* 2025;207:106136.
7. Felician FF, Xia C, Qi W, Xu H. Collagen from Marine Biological Sources and Medical Applications. *Chem Biodivers* 2018; 15(5):e1700557.
8. Amirrah IN, Lokanathan Y, Zulkiflee I, Wee M, Motta A, Fauzi MB. A Comprehensive Review on Collagen Type I Development of Biomaterials for Tissue Engineering: From Biosynthesis to Bioscaffold. *Biomedicines* 2022;10(9):2307.
9. Shoulders MD, Raines RT. Collagen structure and stability. *Annu Rev Biochem* 2009;78:929-58.
10. Gutierrez-Canul CD, Can-Herrera LA, Ramirez-Rivera EJ, Prinyawiwatkul W, Sauri-Duch E, Moo-Huchin VM, *et al.* A Review of Classical and Rising Approaches the Extraction and Utilization of Marine Collagen. *BioTech (Basel)* 2025;14(2)26.
11. Tang J, Saito T. Biocompatibility of Novel Type I Collagen Purified from Tilapia Fish Scale: An *In Vitro* Comparative Study. *Biomed Res Int* 2015;2015:139476.
12. Jafari H, Lista A, Siekapen MM, Ghaffari-Bohloul P, Nie L, Alimoradi H, *et al.* Fish Collagen: Extraction, Characterization, and Applications for Biomaterials Engineering. *Polymers (Basel)* 2020;12(10):2230.
13. Espinales C, Romero-Peña M, Calderón G, Vergara K, Cáceres PJ, Castillo P. Collagen, protein hydrolysates and chitin from by-products of fish and shellfish: An overview. *Heliyon* 2023;9(4):e14937.
14. Jeevithan E, Bao B, Bu Y, Zhou Y, Zhao Q, Wu W. Type II collagen and gelatin from silvertip shark (*Carcharhinus albimarginatus*) cartilage: isolation, purification, physicochemical and antioxidant properties. *Mar Drugs* 2014;12(7):3852-73.
15. Yamamoto K, Igawa K, Sugimoto K, Yoshizawa Y, Yanagiguchi K, Ikeda T, *et al.* Biological safety of fish (tilapia) collagen. *Biomed Res Int* 2014;2014:630757.
16. Nesreen A. Molecular dynamics simulations of the proline and hydroxyproline of collagen. *Multidiscip tud* 2024;14(1):71-82.
17. Leonard AR, Cumming MH, Ali MA, Cabral JD. Fish Collagen Cross-Linking Strategies to Improve Mechanical and Bioactive Capabilities for Tissue Engineering and Regenerative Medicine. *Adv Funct Mater* 2024;34(45):2405335.
18. Jiang YH, Lou YY, Li TH, Liu BZ, Chen K, Zhang D, *et al.* Cross-linking methods of type I collagen-based scaffolds for cartilage tissue engineering. *Am J Transl Res* 2022;14(2):1146-59.
19. Ullah S, Zainol I. Fabrication and applications of biofunctional collagen biomaterials in tissue engineering. *Int J Biol Macromol* 2025;298:139952.
20. Hamman JH. Composition and applications of Aloe vera leaf gel. *Molecules* 2008;13(8):1599-616.
21. Songsiripradubboon S, Kladkaew S, Trairatvorakul C, Sangvanich P, Soontornvipart K, Banlunara W, *et al.* Stimulation of Dentin Regeneration by Using Acemannan in Teeth with Lipopolysaccharide-induced Pulp Inflammation. *J Endod* 2017;43(7):1097-103.
22. Thant AA, Ruangpornvisuti V, Sangvanich P, Banlunara W, Limcharoen B, Thunyakitpisal P. Characterization of a bioscaffold containing polysaccharide acemannan and native collagen for pulp tissue regeneration. *Int J Biol Macromol* 2023;225:286-97.
23. Trinh HA, Dam VV, Banlunara W, Sangvanich P, Thunyakitpisal P. Acemannan Induced Bone Regeneration in Lateral Sinus Augmentation Based on Cone Beam Computed Tomographic and Histopathological Evaluation. *Case Rep Dent* 2020;2020:1675653.
24. Bai Y, Niu Y, Qin S, Ma G. A New Biomaterial Derived from Aloe vera-Acemannan from Basic Studies to Clinical Application. *Pharmaceutics* 2023;15(7):1913.
25. Movasaghi Z, Rehman S, ur Rehman DI. Fourier transform infrared (FTIR) spectroscopy of biological tissues. *Appl Spectrosc Rev* 2008;43(2):134-79.
26. Tatulian SA. FTIR Analysis of Proteins and Protein-Membrane Interactions. *Methods Mol Biol* 2019;2003:281-325.
27. Nalinanon S, Benjakul S, Visessanguan W, Kishimura H. Use of pepsin for collagen extraction from the skin of bigeye snapper (*Priacanthus tayenus*). *Food Chemistry* 2007;104(2):593-601.
28. Bryan MA, Brauner JW, Anderle G, Flach CR, Brodsky B, Mendelsohn R. FTIR studies of collagen model peptides: complementary experimental and simulation approaches to conformation and unfolding. *J Am Chem Soc* 2007;129(25):7877-84.
29. Gong Y, Chen X, Wu W. Application of fourier transform infrared (FTIR) spectroscopy in sample preparation: Material characterization and mechanism investigation. *Adv Sample Prep* 2024;11:100122.
30. Kong J, Yu S. Fourier transform infrared spectroscopic analysis of protein secondary structures. *Acta Biochim Biophys Sin (Shanghai)* 2007;39(8):549-59.
31. Keselowsky AG, Collard DM, Garcia AJ. Surface chemistry modulates focal adhesion composition and signaling through changes in integrin binding. *Biomaterials* 2004;25(28):5947-5954.
32. Riaz T, Zeeshan R, Zarif F, Ilyas K, Muhammad N, Safi SZ, *et al.* FTIR analysis of natural and synthetic collagen. *Appl Spectrosc Rev* 2018;53(9):703-46.
33. Dong Y, Dai Z. Physicochemical, Structural and Antioxidant Properties of Collagens from the Swim Bladder of Four Fish Species. *Mar Drugs* 2022;20(9):550.
34. Skopinska-Wisniewska J, Tuszyńska M, Olewnik-Kruszkowska E. Comparative Study of Gelatin Hydrogels Modified by Various Cross-Linking Agents. *Materials (Basel)* 2021;14(2):396.

35. Bou-Akl T, Banglmaier R, Miller R, VandeVord P. Effect of crosslinking on the mechanical properties of mineralized and non-mineralized collagen fibers. *J Biomed Mater Res A* 2013;101(9):2507-14.
36. Davidenko N, Schuster CF, Bax DV, Raynal N, Farndale RW, Best SM, *et al.* Control of crosslinking for tailoring collagen-based scaffolds stability and mechanics. *Acta Biomaterialia* 2015;25:131-42.
37. Suzuki A, Kodama Y, Miwa K, Kishimoto K, Hoshikawa E, Haga K, *et al.* Manufacturing micropatterned collagen scaffolds with chemical-crosslinking for development of biomimetic tissue-engineered oral mucosa. *Sci Rep* 2020;10(1):22192.
38. Gonçalves PR, Penha RS, Cardoso JJ, Guimarães AR, Bezerra CWB. Green and Effective: Chitosan Blends with Fish Collagen and Aloe vera Exudate. *J Braz Chem Soc* 2024;36(4):e-20240184.
39. Sularsih S, Mulawarmanti D, Rahmitasari F, Siswodihardjo S. In Silico Analysis of Glycosaminoglycan-Acemannan as a Scaffold Material on Alveolar Bone Healing. *Eur J Dent* 2022;16(3):643-7.
40. Jettanacheawchankit S, Sasithanasate S, Sangvanich P, Banlunara W, Thunyakitpisal P. Acemannan stimulates gingival fibroblast proliferation; expressions of keratinocyte growth factor-1, vascular endothelial growth factor, and type I collagen; and wound healing. *J Pharmacol Sci* 2009;109(4):525-31.